

Fragility Assessment for Torsionally Asymmetric Buildings in Plan

S. Feli, S. Tavousi Tafreshi, A. Ghasemi

Abstract—The present paper aims at evaluating the response of three-dimensional buildings with in-plan stiffness irregularities that have been subjected to two-way excitation ground motion records simultaneously. This study is broadly-based fragility assessment with greater emphasis on structural response at in-plan flexible and stiff sides. To this end, three type of three-dimensional 5-story steel building structures with stiffness eccentricities, were subjected to extensive nonlinear incremental dynamic analyses (IDA) utilizing Ibarra-Krawinkler deterioration models. Fragility assessment was implemented for different configurations of braces to investigate the losses in buildings with center of resisting (CR) eccentricities.

Keywords—Ibarra Krawinkler, fragility assessment, flexible and stiff side, center of resisting.

I. INTRODUCTION

THE fragility curves, used for the assessment of seismic losses, are in increasing demand, both for pre-earthquake disaster planning and post-earthquake recovery and retrofitting programs. This is due to the difficulties associated with analyzing individual structures and the importance of obtaining a global view of anticipated damage or effects of intervention, before and after an earthquake, respectively. Analytically derived, mechanics-based fragility relationships result in reduced bias and increased reliability of assessments compared to the fragilities based on post-earthquake observations or on expert opinion [1]. In previous studies [2]-[4] framework of probabilistic structural evaluation process under seismic excitations have been set up. In those studies, different point of views for probabilistic structural assessment process such as the manner in which the hazard should be considered and also the way that structural model should be defined for different stages from the elastic to plastic phases and performance criteria all have been discussed properly. On the other hand, “flexible side” and “stiff side” have been brought up for further analyses of in-plan asymmetric buildings. The corner side that is located farther from the stiffness center is stated as a “flexible side” while the opposite side is stated as a “stiff side”. These corner sides have significant importance in terms of analyzing procedure. In general terms, irregularity conditions occur whenever non-coincident center of mass and CR get involved in process. According to above-mentioned statements, there are two

different conditions have been considered for eccentric (or asymmetric) systems. Firstly, the center of mass (CM) moves from the fixed CR and this is due to non-uniform distribution of mass in plan. Secondly, CR moves from fixed CM and this is due to different distribution of resisting elements along the plan. In this research, braces with different positions have been proposed for further investigations. In the recent seismic disasters, inappropriate response of torsionally-imbalanced buildings has been one of the main reasons for structural collapses and failures [6]. In these buildings, the distribution of seismic demands in the structure is non-uniform and the displacement demands on the elements that are well-known as “stiff side” are absolutely different from those on the “flexible side” [7], [8]. As a result of dynamic excitation, the response of coupled lateral-torsional buildings fundamentally will be different from the structures in which these impacts are negligible. Hence, fragility assessments are carried out to observe the vulnerability of structures that are torsionally imbalanced in their plan.

II. MATERIAL & METHODS

A. General Characteristics of the Structural Models

For the purpose of this study, three steel building with typical architectural characteristics but with different configuration of braces, as shown in Figs. 1-3 are considered. These models are classified as torsionally-imbalanced buildings in their plan. All buildings are five-story and three-span by three-span steel moment frame in one direction and steel moment frame with special concentric braces in another direction, were designed based on AISC 360-05/LRFD provisions. Bay lengths are the same in perpendicular directions. All stories have typical heights equal to 3.2 meters. Dead and live loads that were assigned to the shell areas are 600 Kg/m² and 200 Kg/m², respectively. For this simulation, high seismic zone has been supposed. Ibarra-Krawinkler deterioration model for steel frame elements as shown in Fig. 4 could be utilized for modeling steel frame structures incorporating two nonlinear concentrated springs at the two ends of each element. All sources of non-linearity effects are, then, lumped at these springs by incorporation of an appropriate plasticity model.

The middle parts of all beam-column elements are supposed to be elastic in all stages of simulation.

Sh. Feli, Ph.D. candidate is with Islamic Azad University, Central Tehran Branch, Tehran, Iran (phone: +98 912 5835883; e-mail: sha.feli.eng@iauctb.ac.ir).

Sh. Tavousi Tafreshi, Prof. Dr. and A. Ghasemi, Prof. Dr., are with Islamic Azad University, Central Tehran Branch, Tehran, Iran (e-mail: sh_tavousi@iauctb.ac.ir, amirabbas55@gmail.com).

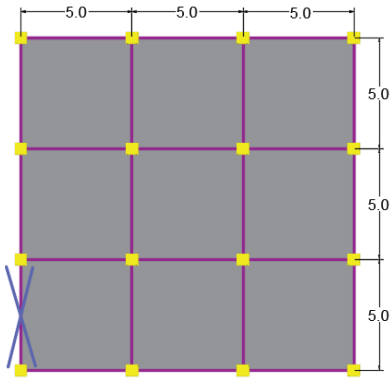


Fig. 1 Typical plan of 1st model

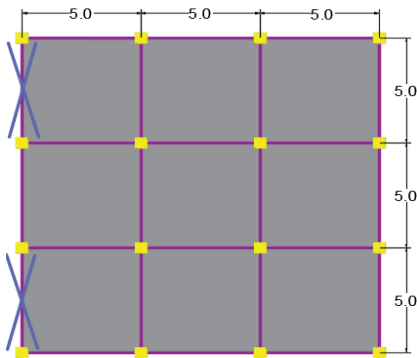


Fig. 2 Typical plan of 2nd model

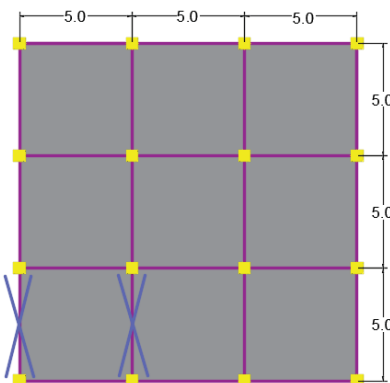


Fig. 3 Typical plan of 3rd model

The utilized final structural model in this study is depicted in Fig. 5. There are seven pairs of ground motion records were adopted from PEER ground motion database and their characteristics are depicted in Table I.

The amount of eccentricities is also illustrated in Table II. And as a result, it is clear that first and third models are asymmetric in both directions; however, the second model is solely asymmetric in one direction and it is symmetric in another direction. Even though it seems to be that the second model has surplus eccentricity in one direction in comparison with others; however, it is symmetric direction is remarkable point of it. Discussion on these findings will be provided in the following sections.

TABLE I
GROUND MOTION RECORDS

Event	Station	Magnitude
Northridge	Anacapa Islands	6.69
Bam	Baft	6.6
Chi-Chi	CHY041	7.62
Loma Prieta	Anderson Dam	6.93
Imperial Valley	Cerro Prieto	6.53
San Fernando	Lake Hughes	6.61
Landers	Fun Valley	7.28

TABLE II
THE AMOUNT OF ECCENTRICITIES IN PLAN

Story	Model	X-Dir ecce	Y-Dir ecce
Roof	1 st	32.64	0.14
5	1 st	33.88	0.22
4	1 st	34.57	0.22
3	1 st	33.38	0.22
2	1 st	29.65	0.22
1	1 st	19.8	0.22
Roof	2 nd	48.65	0
5	2 nd	47.61	0
4	2 nd	46.66	0
3	2 nd	46.27	0
2	2 nd	41.63	0
1	2 nd	30.8	0
Roof	3 rd	25.73	0.28
5	3 rd	26	0.45
4	3 rd	26.16	0.46
3	3 rd	25.54	0.45
2	3 rd	23.56	0.44
1	3 rd	17.63	0.43

All eccentricities are mentioned in percentage.

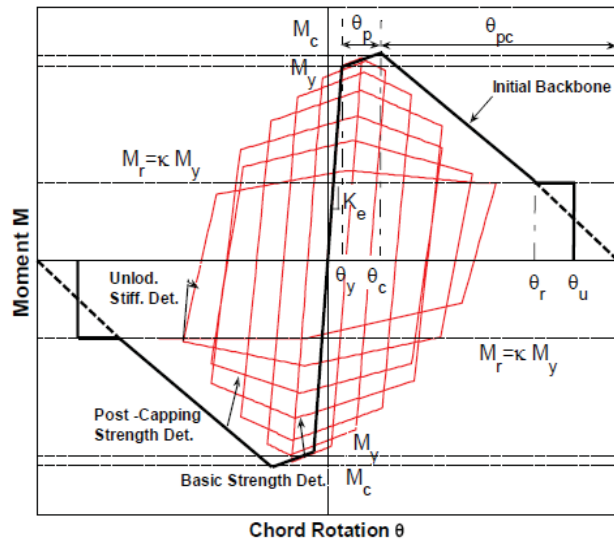


Fig. 4 Modified Ibarra Krawinkler Deterioration Model

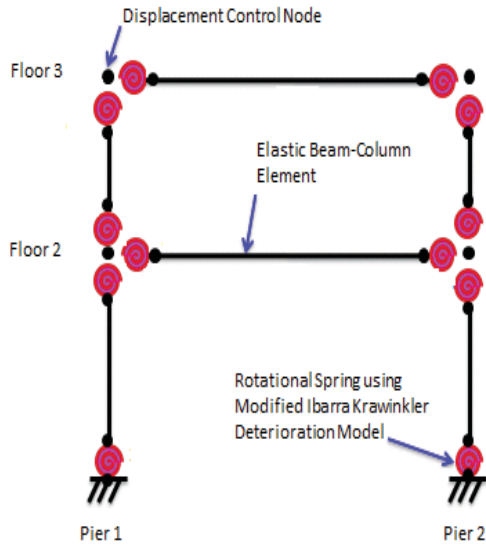


Fig. 5 Final proposed model

III. ANALYTICAL METHODS

For the analytical process of this research, IDA has been carried out [5], [9]. Then, responses of all models were evaluated at the CR, the stiff and the flexible sides of the plan [10]-[12]. According to PEER ground motion database, seven pairs of horizontal ground motion records for orthogonal directions have been selected. Due to the high number of nonlinear analysis runs, the Newton Line Search algorithm (OpenSees, [13]) was utilized for solving the large systems of nonlinear equations usually encountered in three-dimensional nonlinear analysis. In all the analyses, the Newmark integration scheme was utilized. In this section, the results of nonlinear incremental time-history analyses and the associated probabilistic calculations are presented for the models with different plan eccentricities. These results include the IDA curves, probability density functions (PDFs) and cumulative density functions (CDFs) of each structural model separately, all calculated from the IDA of nonlinear models. IDA curves have been drawn as the peak ground acceleration in the direction of interest vs. the maximum inter-story drift observed in that direction for each ground motion of increasing intensity. Figs. 6 (a) and 6 (b) Depicted typical results of IDAs for second model at its stiff side.

IV. FRAGILITY ANALYSIS PROCEDURE

Once IDA analysis is done, fragility curves can be derived subsequently. These curves are representing the probability of exceedance versus peak ground acceleration [14]-[16].

In this section, fragility curves are derived for different configuration of steel braces. Prior to the subjects that have been stated previously, an engineering demand parameters and damage states are needed to be defined. According to HAZUS technical manual [17], four different damage states have been defined which their brief details are depicted in Table III.

Figs. 7 and 8 depict the CDFs and (termed as fragility

curves in structural applications) derived for each building model. The curves represent the probability of exceedance on a specific value of peak ground acceleration in direction of interest; i.e. $P_{\text{exceedance}} | \text{PGA}_x=x$ or $P_{\text{exceedance}} | \text{PGA}_y=y$. In these figures, CDFs have been drawn both for x and y directions, separately.

The slope of curves is an indicator of the uncertainties. Generally, fragility curves are flatter for buildings with high degrees of uncertainty in response compared with structures in which uncertainties in their response are lower.

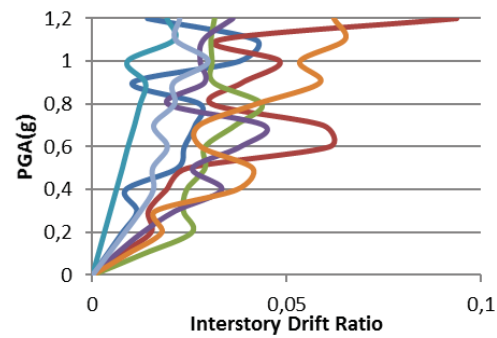


Fig. 6 (a) IDA Curves for second model; X-dir

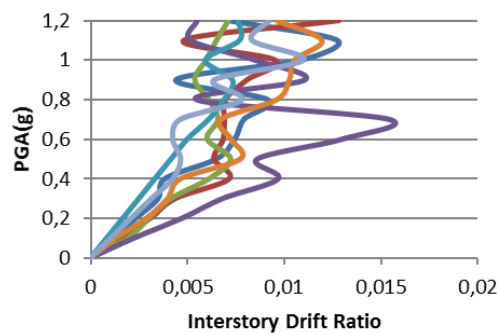


Fig. 6 (b) IDA Curves for second model; Y-dir

TABLE III
ENGINEERING DEMAND PARAMETERS

	No.	Damage states	Interstory Drift
Mid-Rise Steel Moment Frame	1	Slight	0.004
	2	Moderate	0.0069
	3	Extensive	0.0157
	4	Complete	0.04
Mid-Rise Steel Brace Frame	1	Slight	0.0033
	2	Moderate	0.0058
	3	Extensive	0.0156
	4	Complete	0.04

Change in the slope and shape of curves are evident for buildings with high eccentricities, especially in Y direction of plan it can be observed obviously. As a comparison, these three models are investigated with each other at their stiff and flexible sides. The results are performed in their direction of interest and appropriate damage state sequences. The fragility curves for first model are illustrated in Fig. 9.

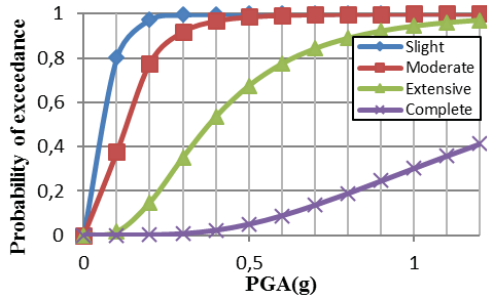


Fig. 7 Fragility Curve for Second Model; X-dir

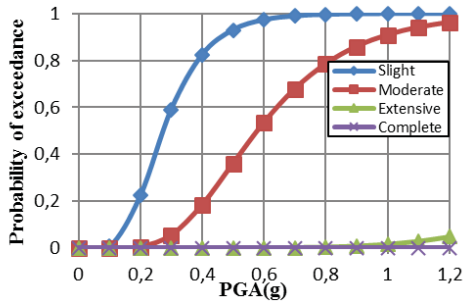
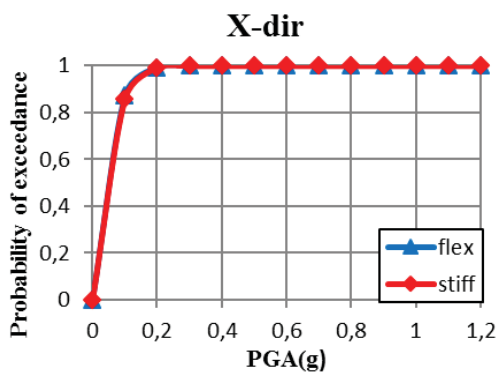


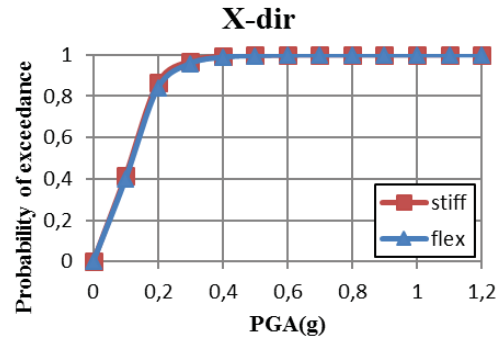
Fig. 8 Fragility Curve for Second Model; Y-dir

It can be clearly concluded that in the X-direction of plan and solely in extensive and complete damage levels, the stiffness side shows a higher vulnerability compared to that of flexible side. However, in the Y-direction of plan remarkable differences can be seen. First of all, flexible side exhibits higher vulnerability compared to that of stiff side and differences in all level of damages can be observed.

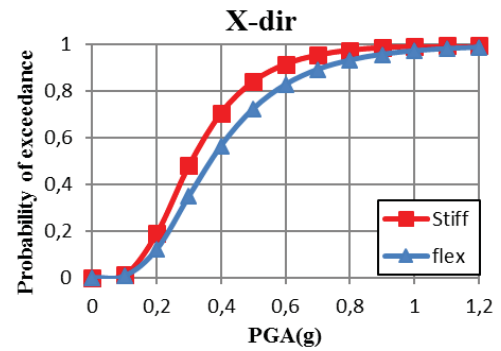
The similar trends can be found for second and third structural models and their fragility curves are shown in Figs. 10 and 11, respectively.



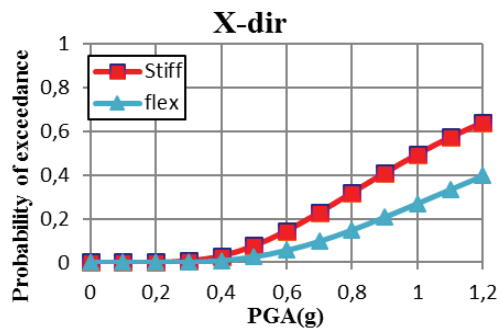
(a) Slight Level of Damage



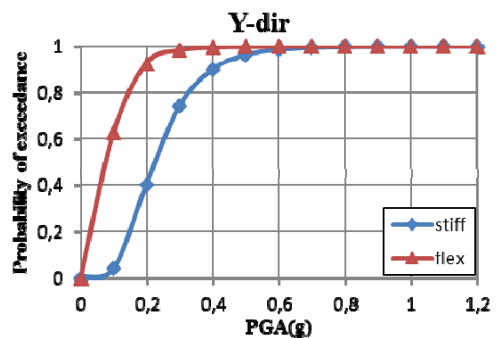
(b) Moderate Level of Damage



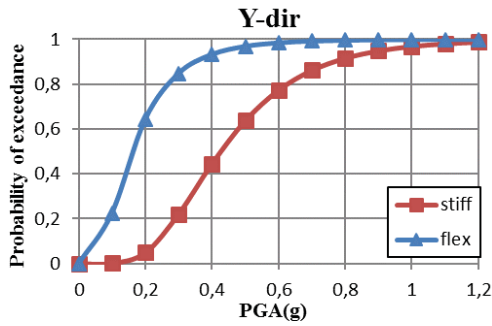
(c) Extensive Level of Damage



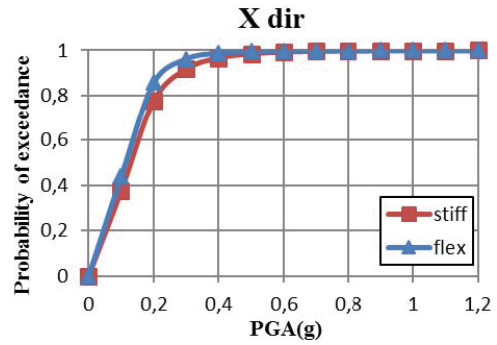
(d) Complete Level of Damage



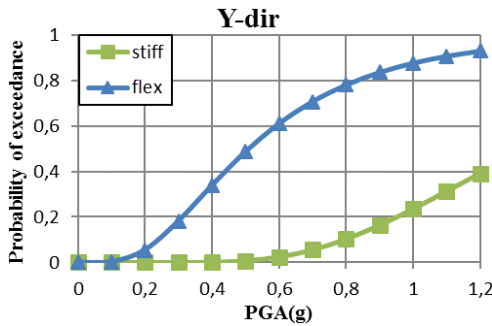
(e) Slight Level of Damage



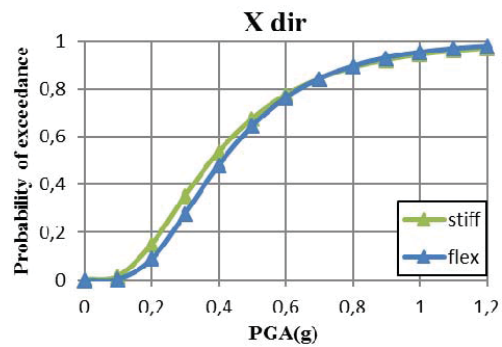
(f) Moderate Level of Damage



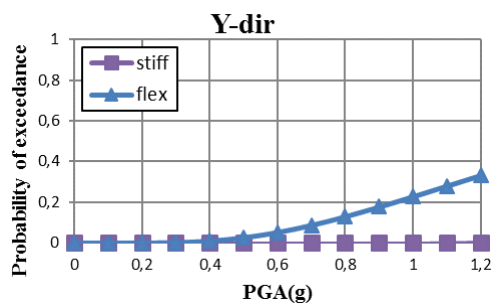
(b) Moderate Level of Damage



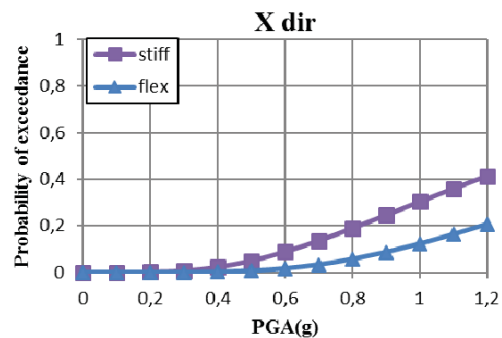
(g) Extensive Level of Damage



(c) Extensive Level of Damage

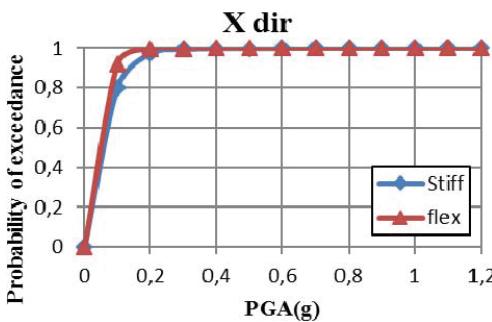


(h) Complete Level of Damage

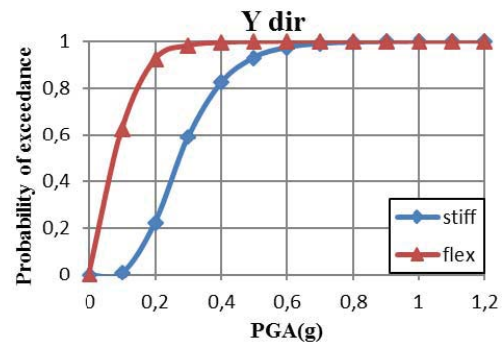


(d) Complete Level of Damage

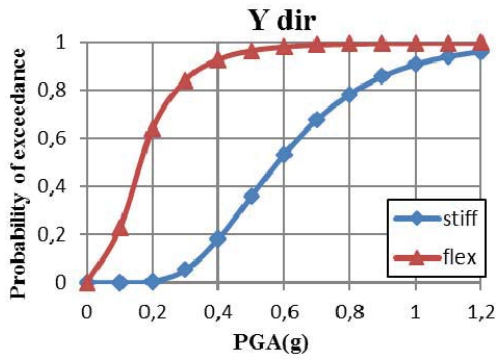
Fig. 9 Comparison of stiff and flexible side of plan for first structural model



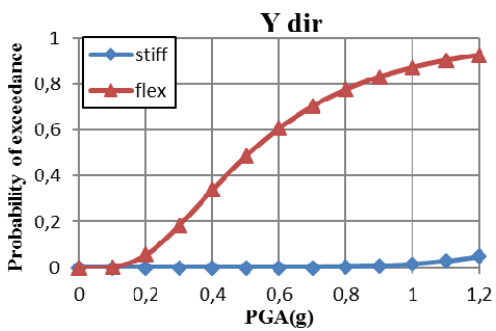
(a) Slight Level of Damage



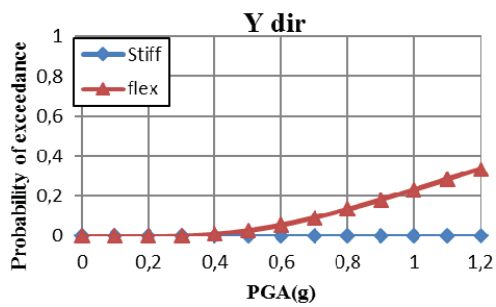
(e) Slight Level of Damage



(f) Moderate Level of Damage

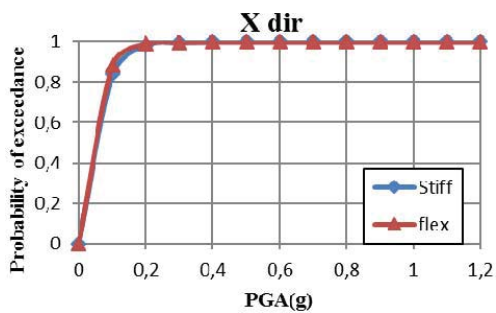


(g) Extensive Level of Damage

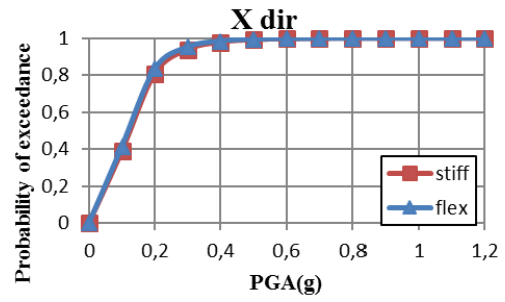


(h) Complete Level of Damage

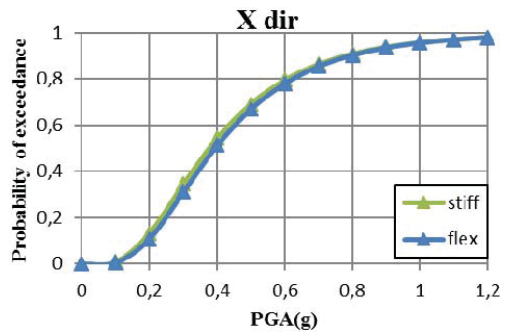
Fig. 10 Comparison of stiff and flexible side of plan for second structural model



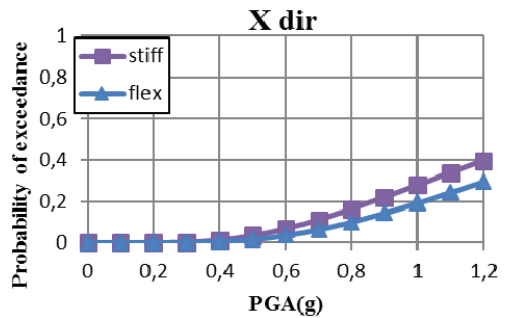
(a) Slight Level of Damage



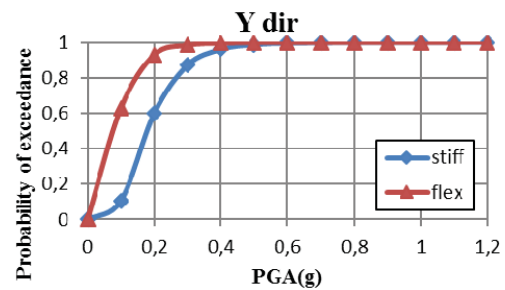
(b) Moderate Level of Damage



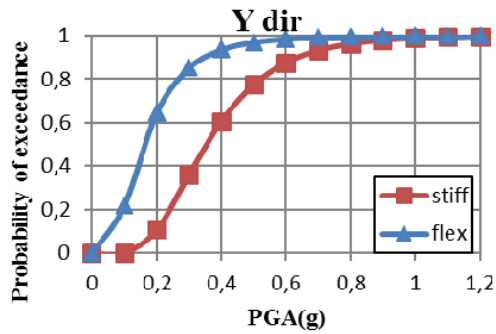
(c) Extensive Level of Damage



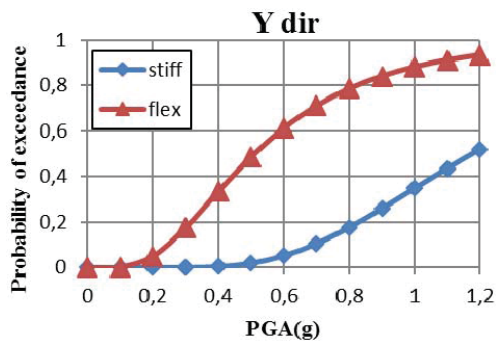
(d) Complete Level of Damage



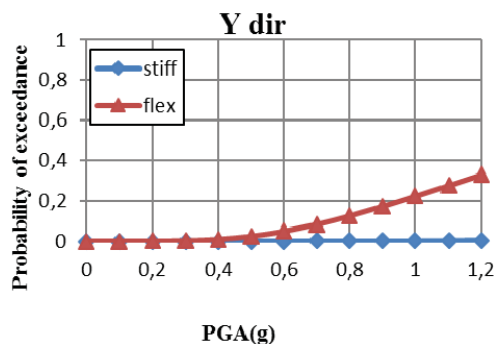
(e) Slight Level of Damage



(f) Moderate Level of Damage



(g) Extensive Level of Damage



(h) Complete Level of Damage

Fig. 11 Comparison of stiff and flexible side of plan for third structural model

V. CONCLUSION

In this study, fragility assessment for torsionally asymmetric buildings in plan for three models with different configurations of braces is presented which CR eccentricities play important role in these cases. The results can be concluded as follows:

- In the component fragility analysis, the second model exhibits a lower fragility compared to that of other sophisticated models, especially it is quite obvious in Y-direction. This verifies that the second model's symmetric direction was fairly dominant on its higher eccentricity. It is also noticeable that the first and third models show a severe vulnerability and that is because of their both directional asymmetric plan.

- In the X-direction of all models, almost level of damages is functioning independently from their stiff and flexible sides which it means that they react same as each other.
- In the complete level of damage, whole models have encountered the most uncertainties which they may demand more ground motion records to receive a comprehensive assessment.

REFERENCES

- [1] National Institute of Building Sciences. Development of a standardized earthquake loss estimation methodology. Washington (DC): FEMA; (1995).
- [2] Jalayer F. "Direct probabilistic seismic analysis: implementing nonlinear dynamic assessments" Ph.D. Dissertation, Department of Civil and Environmental Engineering, Stanford University, Stanford, California, (2003).
- [3] Ibarra LF, Medina RA, Krawinkler H. "Hysteretic models that incorporate strength and stiffness deterioration." International Journal for Earthquake Engineering and Structural Dynamics, Vol. 34, No.12, pp. 1489-1511 (2005).
- [4] Zareian F, Medina RA. "A practical method for proper modeling of structural damping in inelastic plane structural systems." Journal of Computers and Structures, 88, 45-53 (2010).
- [5] Vamvatsikos D, Cornell CA. Tracing and post-processing of IDA curves: Theory and software implementation, Report No. RMS-44, RMS Program, Stanford University, Stanford (2001).
- [6] Mario de Stefano, Barbara Pintucchi, "A review of research on seismic behavior of irregular building structures" (2008).
- [7] Paulay T. "Some Design Principles relevant to Torsional Phenomena in Ductile Buildings". Journal of Earthquake Engineering, 5:3, 273-308 (2001).
- [8] Wong CM, Tso WK. "Inelastic seismic response of torsionally unbalanced systems designed using elastic dynamic analysis". Earthquake Engineering and Structural Dynamics, 23, 7, pp. 777-79 (1994).
- [9] Dimitrios Vamvatsikos, Allin Cornell, Incremental Dynamic Analysis, John Wiley & Sons (2002).
- [10] Haj seiyed Taghia, Abdoreza S. Moghadam, Ashtiany, Seismic performance of torsionally stiff and flexible multi-story concentrically steel braced buildings, (2012).
- [11] Salar manic, Abdoreza S. Moghadam, Ashtiany, Probabilistic Response Evaluation of Plan-Irregular Buildings Subjected to Bi-directional Seismic Loading, (2014).
- [12] Yasser picazo, Orlando Diaz Lopez, Luis Esteva, Seismic reliability analysis of buildings with torsional eccentricities, (2014).
- [13] Silvia Mazzoni, Frank McKenna, Michael H. Scott, Gregory L. Fenves et al. 2007, Open System for Earthquake Simulation(OPENSEES) Language Manual
- [14] Barron-Corvera, 2000, Spectral Evaluation of Seismic Fragility in Structures
- [15] Keith Porter, Ron Hamburger, Practical Development and Application of Fragility Functions, (2007).
- [16] Seong hoon, amr Elnashai, Fragility relationships for torsionally-imbalanced buildings using three-dimensional damage characterization, (2006).
- [17] Multi-Hazard Loss Estimation Methodology Earthquake Model, HAZUS MR4, Technical Manual